Journal of Earth Science, 2016 online *ISSN 1674-487X*
Printed in China
DOI: 10.1007/s12583-016-0909-8

Paleogeothermal reconstruction and thermal evolution of the source rocks in the Puguang gas field, Northeastern Sichuan Basin

Chuanqing Zhu[1,2]*, **Nansheng Qiu**[1,2], **Huanyu Cao**[3], **Song Rao**[4], **Shengbiao Hu**[5]

1. *State Key Laboratory of Petroleum Resources and Prospecting, China University of Petroleum, Beijing* 102249, *China*
2. *College of Geosciences, China University of Petroleum, Beijing* 102249, *China*
3. *Exploration branch, SINOPEC, Chengdu* 610041, *China*
4. *College of Geosciences, Yangtze University, Jingzhou* 434023, *China*
5. *State Kay Laboratory of Lithospheric Evolution, Institute of Geology and Geophysics, Chinese Academy of Sciences, Beijing* 100029, *China*

ABSTRACT: The thermal history and organic matter maturity evolution of the source rocks of boreholes in the Puguang gas field were reconstructed. An integrated approach based on vitrinite reflectance and apatite fission track data was used in the reconstruction. Accordingly, the geothermal conditions of gas accumulation were discussed in terms of the geological features of reservoirs in the northeastern Sichuan basin. The strata reached their maximum burial depth in the late Cretaceous era and were then uplifted and denuded continuously to the present day. The geothermal gradient and heat flow in the late Cretaceous era were approximately 30.0 °C/km and 66 mW/m^2, respectively, which were both higher than those at present. The tectonothermal evolution from the late Cretaceous era to the present is characterized by denudation and cooling processes with an erosion thickness of ~2.7 km. In addition to the Triassic era, the Jurassic era represents an important hydrocarbon generation period for both Silurian and Permian source rocks, and the organic matter maturity of these source rocks entered into a dry gas period after oil generation. The thermal conditions are advantageous to the accumulation of conventional and unconventional gas because the hydrocarbon generation process of the source rocks occurs after the formation of an effective reservoir cap. In particular, the high geothermal gradient and increasing temperature before the denudation in the late Cretaceous era facilitated the generation of hydrocarbons, and the subsequent cooling process favored its storage.

KEY WORDS: Paleogeothermal reconstruction; Apatite fission track; Vitrinite reflectance; Thermal evolution of source rocks; Puguang gas field.

0 INTRODUCTION

The thermal states of basins affect the hydrocarbon generation, migration, and accumulation processes; therefore, reconstructing basin thermal history is significant for petroleum accumulation analyses. The maturity of organic matter is primarily controlled by the temperature of the source rock (Tissot and Welte, 1984; Tissot and Pelect, 1987). Given the geothermal dependence of hydrocarbon generation, several researchers consider geotherm as another main controlling factor for oil and gas accumulation in addition to the source rocks. According to "Con-control by source and heat" theory (Zhang, 2012), the thermal field type determines the heating intensity of a basin or source rock, and the different thermal evolutionary histories of hydrocarbon source rocks are controlled by the thermal background of the basin and the burial history of the source rocks (Zhang, 2012; Zhang, 2014).

The northeastern Sichuan produces a large amount of natural gas in the basin of various regions, including the Puguang and Yuanba gas fields. The thermal history of these regions has been investigated following its exploration and exploitation. However, existing studies have mainly reconstructed the thermal history of these regions using single methods. For instance, vitrinite reflectance and thermophysical property data were employed to simulate the thermal history or hydrocarbon source rock history, and the results indicated that the paleo-heat flow reached its maximum values (62 mW/m^2 to 70 mW/m^2) around 255 Ma, then began to decrease until the present. The maximum erosion occurred on the Mesozoic–Cenozoic unconformity and reached approximately 2100 m (Lu et al., 2005). Moreover, the apatite fission track (AFT) and (U-Th)/He methods have been used to study uplift and denudation history (Shen et al., 2007; Mei et al., 2010; Tian et al., 2011; Tian et al., 2012). Three possible cooling histories have been determined, namely, linear cooling since 100 Ma,

*Corresponding author: zhucq@cup.edu.cn

Manuscript received March 16, 2015.
Manuscript accepted March 14, 2016.

Zhu, C. Q., Qiu, N. S., Cao, H. Y., et al., 2016. Paleogeothermal reconstruction and thermal evolution of the source rocks in the Puguang gas field, Northeastern Sichuan Basin. *Journal of Earth Science*, *online*. doi: 10.1007/s12583-016-0909-8. http://en.earth-science.net

enhanced cooling since 40 Ma following slow cooling since 100 Ma, and enhanced cooling since 30 Ma following slow cooling since 100 Ma. The total post-early Cretaceous denudation for the northeastern Sichuan Basin is estimated at 5 km (Tian et al., 2011). Although geothermal thermochronometry and vitrinite reflectance data were simultaneously considered in analyzing the thermal history or thermal evolution of source rocks, only the thermal history was emphasized in literature (Qiu et al., 2008) and maturity was forward modeled using estimated parameters (Rao et al., 2011; Wu and Peng, 2013). Consequently, the denudation process (erosion thickness and periods) and the paleogeothermal gradient before denudation, which are dominant factors in the thermal evolution of source rocks, have not been discussed in detail. This study combines vitrinite reflectance and AFT data to reconstruct the thermal history and evolution of source rocks in Puguang boreholes. The geological features of oil and gas accumulation, as well as the geothermal conditions of natural gas accumulation in this region, are discussed.

1 GEOLOGICAL BACKGROUND

The northeastern Sichuan area is located in front of the Micang–Daba Mountain arcuate tectonic zone in the northeastern part of the Sichuan Basin to the south of the Micang Mountain bulge (Figure 1). The eastern Sichuan fold–thrust belt is the main structure in this region (Zheng et al., 2008). Marine carbonate was primarily deposited during the Neopaleozoic era, and thick foreland basin sediment was deposited during the Mesozoic era. As a consequence of the Caledonian movement, Devonian–Lower Carboniferous strata were rarely formed in this region and Middle Jurassic strata were uplifted to the surface.

The strata in northeastern Sichuan include multiple combinations of reservoir formation systems vertically, which provide advantageous conditions for hydrocarbon accumulation. Four sets of marine source rocks were developed in this region, including the lower Cambrian Niutitang formation, Upper Ordovician Wufeng–Lower Silurian Longmaxi formation, Lower Permian formation, and Upper Permian formation (Huang et al., 1996; Liang et al., 2008; Tenger et al., 2010; 2012). The hydrocarbon of the Puguang gas field primarily originates from Permian and Silurian (mostly Permian) source rocks (Cai et al., 2005; Ma et al., 2007a; Ma, 2010; Tenger et al. 2012).

The reservoir strata of the Puguang gas field are mainly combinations of reef flat-dolomite in the margin of the Permian Changxing formation (Pch) platform and a deposited grain shoal-oolitic beach of the shallow sea-open platform facies of the Triassic Feixianguan formation (T1f). Gypsum salt rocks were developed in sections 2 and 4 of the Lower Triassic Jialingjiang formations (T1j) and in section 2 of the Leikoupo formation (T2l) during the mid-Triassic era and served as the seal rocks of the natural gas reservoir in the Changxing–Feixianguan formations of the Puguang gas field (Ma et al., 2007a; 2007b. in Figure 2).

2 DATA AND PALEO-THERMAL RECONSTRUCTION

2.1 Paleogeothermal indicator data

Vitrinite reflectance (Ro) and AFT are the most commonly used indicators for paleotemperature reconstruction. Ro is the most commonly used indicator for organic matter maturity and can be used to reveal the maximum paleotemperature. Although the annealing kinetics of various apatite grains slightly differ from one another, the annealing threshold is set to ~60 °C, while the full annealing temperature ranges between >120 °C and ~150 °C (Gleadow et al., 1983; Green et al., 1985, 1986; Armstrong et al., 1997; Ketcham et al., 1999; Armstrong, 2005; Ketcham, 2005). Given this annealing behavior, the AFT data can be used to reconstruct the thermal evolution of the samples, especially the paleotemperature history in the AFT partial annealing zone (PAZ), which ranges between ~60 °C and 125 °C (Gleadow et al., 1983).

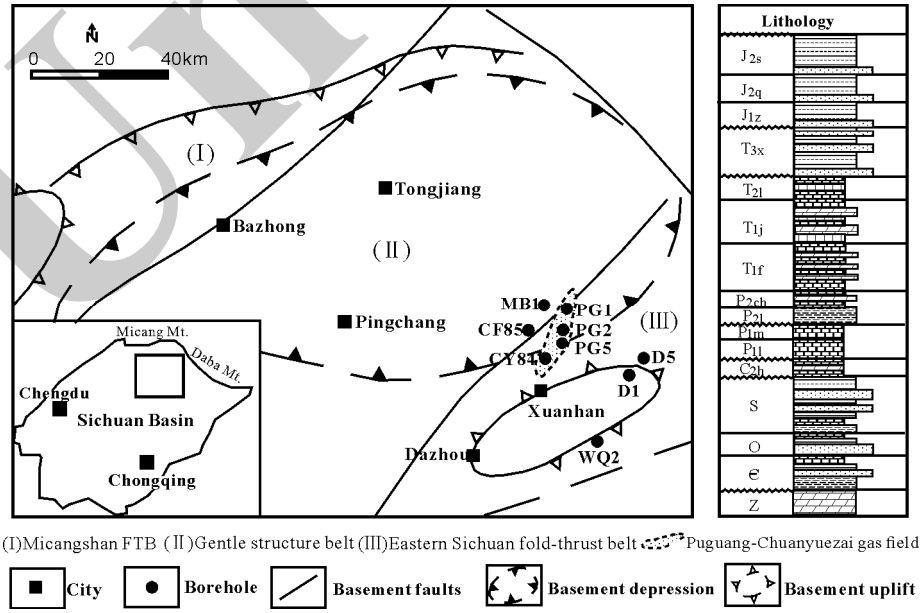

Figure 1. Distribution of boreholes, sketch of basement structures, and strata column of the northeastern Sichuan basin (modified from Rao et al., 2011).

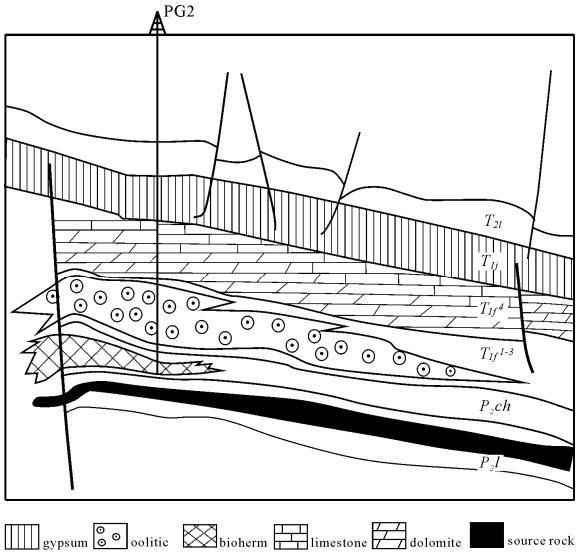

Figure 2 Cross-section of the Puguang 2 gas reservoir (modified from Ma et al., 2007).

geothermal gradient in this area (~20 °C/km), the temperatures of samples PG2-5, PG2-6, and PG5-1 (with mean track lengths of 12.10 ± 1.8 μm, 12.0 ± 1.65 μm, and l2.1 ± 1.9 μm, respectively) are lower than the threshold temperature (~60 °C) at which the AFT commenced annealing. By contrast, the temperatures of samples PG5-8 and PG5-9 (with mean track lengths of 10.3 ± 2.2 μm and 11.2 ± 2.0 μm, respectively) were in the range of the partial annealing zone of the current AFT.

The Ro values of PG 2 and PG5 are between 1.3% and 2.5%, and the Jurassic Ro values are between 1.3% and 2.0%, which indicates that the Jurassic Ro is in the high maturity stage. The Triassic Ro values are all > 2.0%, which suggests that the Triassic Ro is in the post-maturity stage. Furthermore, at a depth of ~2500 m to 3500 m, the Ro values and increasing gradients of PG2 and PG5 become consistent.

2.2 Paleogeothermal reconstruction methods

Thermal history can be reconstructed using paleogeothermal indicators, such as low-temperature thermochronologic data (i.e., AFT and (U-Th)/He), and organic matter maturity indicators (i.e., Ro), such as stochastic

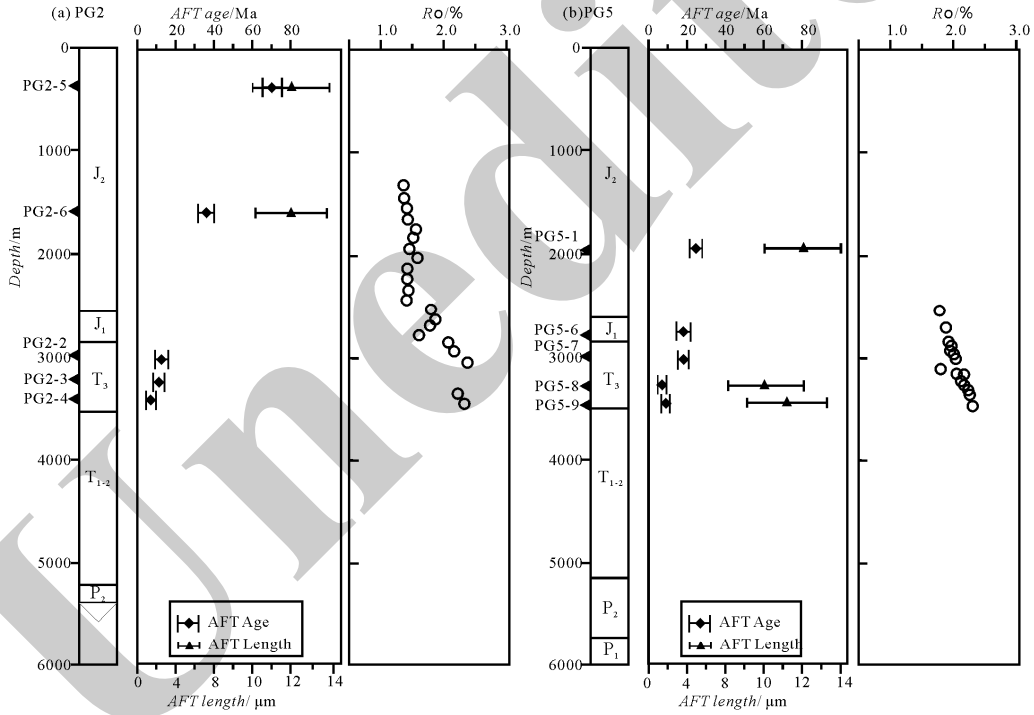

Figure 3 AFT and Ro data of the samples of the Puguang boreholes.

The AFT data (Table 1 and Figure 3) of Puguang boreholes are mainly sampled at depths above 3500 m. The AFT age of the upper sample of PG2 (PG2-5, depth = 370 m) is 70.2 ± 5.1 (1σ) Ma. Given that the depth increases along with age, the fission track age of PG2-4 reaches 8.5 ± 1.1 (1σ) Ma at ~3500 m, and the AFT age of PG5 samples demonstrate the same feature. Moreover, the fission track ages of all samples are less than the strata ages, which suggests that the tracks of samples have experienced annealing. Based on the current inversion (Lutz and Omar, 1991; Corrigan, 1991; Gallagher, 1995), paleotemperature gradient-based inversion (Duddy et al., 1991; Bray et al., 1992; O'Sullivan, 1999; Hu et al., 2007), and paleo-heat flow-based inversion (Lerche et al., 1984; Qiu et al., 2004). We employed the stochastic inversion for the AFT data and the paleotemperature gradient-based inversion for the Ro data to reconstruct the paleogeothermal history and determine the erosion thickness. We then modeled the thermal evolution and hydrocarbon generation history of the source rocks using

Table 1 Apatite fission track data from PG2 and PG5 boreholes *

No.	Depth (m)	Strata	NG	ρ_s (10^5/cm^2) (Ns)	ρ_i (10^5/cm^2) (Ni)	ρ_d (10^5/cm^2) (Nd)	P(χ^2) (%)	Central age ±1 σ (Ma)	L(μm) (NL)
PG2-2	3025.9	T_{3x}	20	1.758 (50)	44.29 (1260)	16.48 (3125)	99.9	12.7±1.9	
PG2-3	3247.1	T_{3x}	21	0.667 (65)	17.54 (1710)	15.39 (3041)	96.2	11.4±1.5	
PG2-4	3415.5	T_{3x}	20	0.761 (44)	32.78 (1895)	14.80 (2988)	77.7	6.7±1.0	
PG2-5	370.0	J_{3p}	21	4.82 (257)	19.82 (1057)	14.92 (2988)	83.8	70.2±5.1	12.10±1.8 (104)
PG2-6	1590.0	J_{2x}	22	4.903 (182)	38.69 (1436)	15.04 (2988)	99.7	37.0±3.0	12.0±1.65 (106)
PG5-1	1972.0	J_{2q}	19	2.435 (192)	3.932 (310)	2.113 (3144)	79.0	24±3	12.1±1.9 (19)
PG5-6	2792.0	J_{1z}	21	1.713 (199)	4.131 (480)	2.113 (3144)	11.3	17±2	
PG5-7	3013.5	T_{3x}	10	2.422 (100)	5.062 (209)	2.029 (3144)	24.5	17±3	
PG5-8	3350.0	T_{3x}	28	0.640 (138)	3.880 (836)	2.134 (3144)	4.4	7.0±0.8	10.3±2.2 (30)
PG5-9	3508.0	T_{3x}	27	0.733 (191)	3.189 (831)	2.008 (3144)	2.7	9.4±1.0	11.2±2.0 (16)

*Notes: No. = Sample Number, N = Number of dated grains, Ns = Number of counted spontaneous tracks; Ni= Number of counted induced tracks; ρ_s = density of spontaneous tracks; ρ_i = density of induced tracks; Nd = Number of tracks on standard glass(CN-5); ρ_d = Density of tracks on standard glass (CN-5); L = Mean track length; NL= Number of measured track lengths. The ages of the PG2 samples which were analyzed in the University of Melbourne (Tian et al., 2011) and calculated using a zeta of 389.3 ± 5.0 for CN5 with 12.2ppm, while the ages of the PG5 samples which were analyzed in China University of Geosciences, Beijing using a zeta of 385.0 ± 12.0.

these inverse results and other geologic parameters, such as the geochemistry of the source rocks and the thermal properties of the strata (Figure 4).

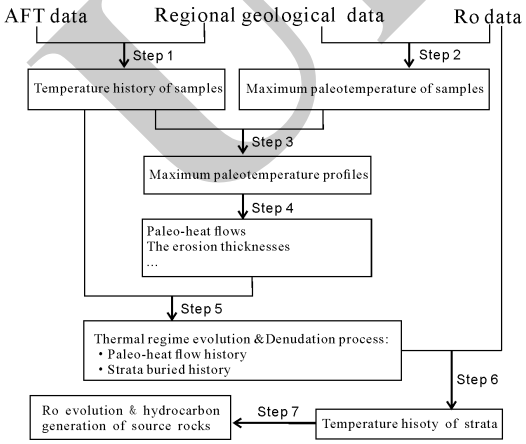

Figure 4 Flowchart of the thermal history modeling process based on AFT and Ro data.

The principles and modeling of the low-temperature thermochronologic methods have been continuously developed and widely introduced (Naeser, 1979; Gleadow et al., 1983; Gleadow, 1981; Gleadow and Fitzgerald, 1987; Fitzgerald and Gleadow, 1990; Fitzgerald et al., 1993; Armstrong et al., 1997; Armstrong, 2005; Ketcham et al., 2007). The thermal history of the samples have been reconstructed via the stochastic inversion method (Corrigan, 1991) and the Monte Carlo method based on the AFT annealing model (Ketcham et al., 2007) using the HeFty v1.7.4 software (Figure 4, step 1).

Many scholars have studied the model dynamics of vitrinite reflectance evolution to obtain the activation energy distributions of different types of kerogen (Tissot and Espitalie, 1975; David and Antia, 1986; Burnham et al., 1989, 1987; Braun and Burnham, 1987; Burnham and Sweeney, 1989; Larter, 1989; Sweeney and Burnham, 1990). Given its maturity and conciseness, The EASY Ro% model (Sweeney and Burnham, 1990) is currently the most-applied model in inversing the maximum paleotemperatures using Ro data because of its maturity and conciseness (Figure 4, step 2).

A series of successive sedimentary strata reach their maximum temperatures simultaneously under stead-state heat conduction conditions. Therefore, based on the maximum

temperatures of a series of samples (Ro or AFT) at different depths, the paleogeothermal gradient can be obtained upon reaching the maximum paleotemperature (Figure 4, step 3). The paleo-heat flow and erosion thickness can also be determined accordingly (Figure 3, step 4).

In contrast to the paleotemperature gradient-based method, AFT modeling can directly estimate the time at which a sedimentary section begins to cool down from its maximum paleotemperature. Therefore, combining Ro with AFT provides a consistent and integrated interpretation of the reconstructed thermal history of the boreholes, the paleogeothermal regime evolution (maximum paleotemperature gradient and heat flow),

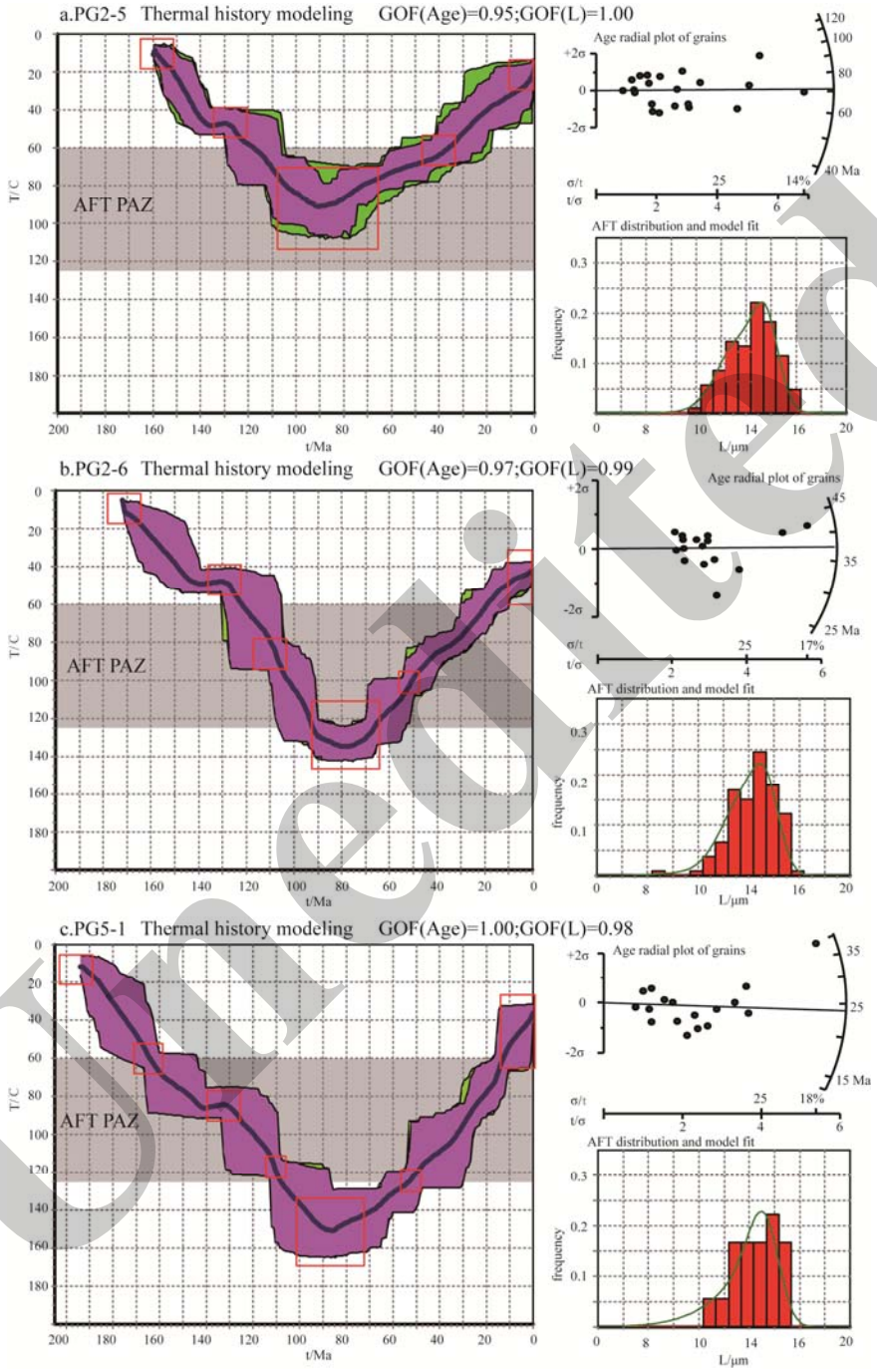

Figure 5 Thermal history modeling results of the AFT samples. A total of 10000 paths have been modeled using the Monte Carlo method. Red line rectangles refer to the sample ages, the present temperature, and other regional geological data. The inversion results are a series of possible or equivalent thermal history paths that constitute a probability-distribution belt. The width and dispersion of the belt depend on the complexity of its thermal history. A more complex thermal history exhibits a wider distribution belt and greater uncertainty. Green regions indicate the envelopes of "accepted traces" ($0.4 \leq GOF < 0.6$), and purple regions indicate the envelopes of "good traces" ($0.6 \leq GOF \leq 1.0$). Blue bold line in each result indicates the mean "good traces." The goodness of fit (GOF) of these results is listed. Green curves indicate the fit of the AFT length distribution.

and the denudation process (uplift period and erosion thickness) (Figure 4, step 5).

Combined with the burial and denudation information from the sample thermal history that is obtained from AFT and by considering the current heat flow as a constraint, the heat flow history of a borehole can be reconstructed using the paleo-heat flow method (Lerche, 1990; Lerche et al., 1984). The geothermal history of the strata is then reconstructed based on the heat flow and strata burial histories (Figure 4, step 6). Based on the Ro evolution dynamic model (i.e. the EASY% Ro model), the maturity evolution and hydrocarbon generation history of the source rocks can be modeled (Figure 4, step 7).

2.3 Paleogeothermal evolution and denudation in Puguang area and thermal evolution of source rocks

2.3.1 Thermal history and erosion thickness

Figure 5 shows the thermal history modeling results for the PG2 and PG5 samples, which are computed based on AFT data. The results for the PG2-5, PG2-6, and PG5-1 samples indicate that after burying these samples and allowing a possible slight cooling between 140 Ma to 130 Ma, the entire process was a continuous burial process before 90 ± 10 Ma. After reaching the maximum paleotemperature at 90 Ma, the cooling commenced and continued, which indicated that the uplift and denudation process of northeastern Sichuan continued since the late Cretaceous era. Given the maximum paleotemperatures of PG2-6 and PG5-1 upon entering the full annealing zone, these two samples and other deeper samples cannot be used to reveal the maximum paleotemperatures. However, the approximate maximum paleotemperatures of PG2-6 and PG5-1 can be estimated because these samples are located around the AFT full annealing zone. These samples experienced their maximum paleotemperatures at ~90 Ma. The maximum temperature of PG2-5 is ~90 °C (indicating excellent traces), which was lower than the full annealing temperature of AFT. Therefore, a relatively accurate buried history and denudation process can be revealed. The strata reached their maximum paleotemperatures (indicating maximum burial depth under a normal thermal evolution) in the late Cretaceous era and were then uplifted and cooled continuously until the present.

Denudation process can be revealed by the cooling history, but the erosion thickness cannot be accurately determined based on low temperature thermalchronology modeling because the paleotemperature gradient cannot be constrained by a single sample. Assuming that the cooling resulted from denudation and occurred under a constant paleothermal gradient of ~20 °C/km (similar to that of the present day), Tian et al. (2011) estimated the total post-early Cretaceous denudation for the northeastern Sichuan Basin at ~5 km. Lu et al. (2005) considered the maximum erosion in the northeastern Sichuan basin that occurred on the Mesozoic–Cenozoic unconformity and obtained a mean of ~2100 m. However, the paleo-heat flow-based modeling result shows that the erosion thickness of PG2 is 2750 m, thereby indicating a huge difference between the results from low temperature thermalchronology modeling and paleo-heat flow-based modeling. However, given that these two studies and other previous works have not presented paleogeothermal gradient results, the accuracy of erosion thickness cannot be evaluated.

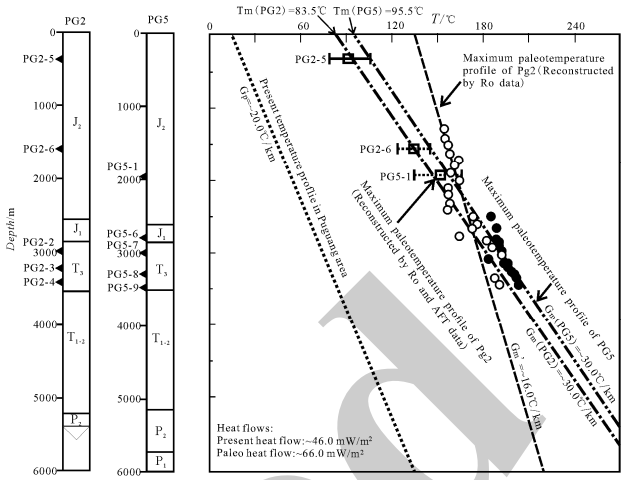

Figure 6 Maximum paleotemperature profile reconstruction of PG2 and PG5 based on both Ro and AFT data. The maximum paleotemperature gradients (Gm) are calculated using the maximum paleotemperatures that are reconstructed based on the Ro and AFT data, while the present temperature gradients (Gp) are calculated using the measurement data in the Puguang area (Lu et al., 2005; Xu et al., 2011). The erosion thickness (E) of PG2 is computed as E(PG2) = [Tm(PG2) – 10°C (paleo-surface temperature)]/Gm(PG2) = ~2.5 km. The erosion thickness of PG5 is computed as E(PG5) = [Tm(PG5) – 10 °C (paleo-surface temperature)]/Gm(PG5) = ~2.9 km. The heat flow (q) values are calculated with the temperature gradient (G) and thermal conductivity (k) of the strata as q = G × k. The present thermal conductivity (k) of the boreholes are the harmonic mean values (~2.31 W/(m•K)) that are calculated based on the measured values (Lu et al., 2005) of the different lithology rocks and their component proportions in the lithological column of boreholes because the paleothermal conductivity can be inversed from the present value, whereas the paleo-porosity and paleo-heat flow can be determined accordingly. The paleotemperature is reconstructed using Thermodeo for Windows 2008.

The inversion results (Ro and AFT data) from the paleogeothermal gradient method (Figure 6) revealed that the paleogeothermal gradient before the denudation was approximately 30.0 °C/km and that the erosion thickness since the late Cretaceous era was approximately 2.7 ± 0.2 km (mean erosion thicknesses of PG2 and PG5). The paleogeothermal gradient was higher than the current values (~20 °C/km) (the heat flow was in the same situation), thereby reflecting the cooling and uplifting processes of the Puguang area since the late Cretaceous era (~90 Ma).

2.3.2 Thermal evolution of the source rocks

Figure 7 shows the reconstructed maturity history of the source rocks of PG2. As a result of the Caledonian movement-driven uplift from the late Silurian to early Carboniferous eras, the lower Silurian source rocks only reached the hydrocarbon generation threshold in the late

Carboniferous era. During the high heat flow period in the late Permian era (~260 Ma) (Zhu et al., 2010a; 2016; Rao et al., 2013), the lower Silurian source rocks further evolved and entered the oil generation peak. The Jurassic era was the most important hydrocarbon generation period for the Permian and Silurian source rocks, and the thermal evolution process entered a post-maturity state (dry gas phase) after experiencing an oil generation peak in the Triassic era. According to Ma et al. (2007a), the Silurian and Permian source rocks reach a hydrocarbon generation threshold in the early Triassic era, the oil generation peak occurs in the early mid-Jurassic era, and the post-maturity evolution state occurs either in the late mid-Jurassic era or the late Jurassic era. Wu and Peng (2013) argued that the Permian source rocks rapidly generate hydrocarbon during the late Triassic and mid-Jurassic eras. Other studies identified the Jurassic era as one of the main hydrocarbon generation periods for the Silurian and Permian source rocks in this region. Given the conflicting consideration on the heat flow history and the denudation process, our proposed time windows of when the source rocks entered the oil threshold and when the hydrocarbon generation was terminated differed from those proposed in previous works. However, our proposed main hydrocarbon generation periods were slightly in agreement with those of previous research.

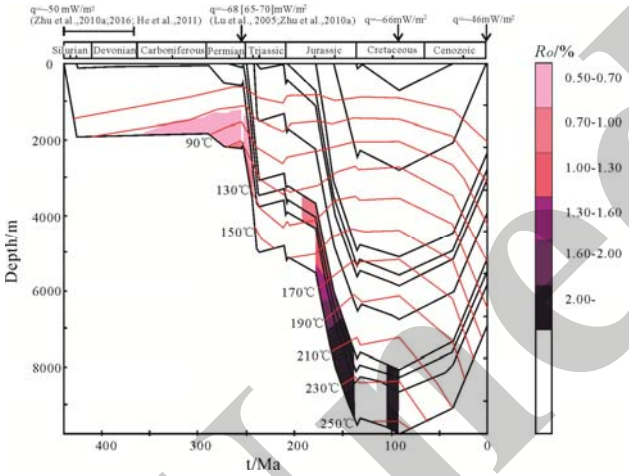

Figure 7 Burial history and thermal evolution of source rocks of Puguang 2. The paleo-heat flows in the late Cretaceous era and the present are imported as the determinate restraints for heat flow history. However, previous works on the paleo-heat flow in the northeastern Sichuan basin (Lu et al., 2005; Zhu et al., 2010a; 2016; He et al., 2011) were considered for the complete evolution.

3. THERMAL EVOLUTION CONDITIONS FOR NATURAL GAS ACCUMULATION

3.1 Hydrocarbon generation period with accumulation

Petroleum accumulation depends on the configuration of hydrocarbon generation as well as the migration, formation, and evolution of the reservoir and seal conditions. The Silurian and Permian source rocks reached their oil and gas generation peaks in the late Triassic era and in the Jurassic era (Figure 8), respectively, which were both later than the formation of the reservoir and seal rocks. The hydrocarbon generation period provided a favorable condition for the accumulation of oil and gas for these Silurian and Permian source rocks. Given the multiple phases of hydrocarbon generation, the Paleozoic source rocks in the northeastern Sichuan basin had more favorable conditions for hydrocarbon accumulation than those in the southwest and other regions (Zhu et al. 2010b).

Evaporation rocks and deeply buried, highly evolved mudstone are the most important oil and gas cap rocks (Zhou et al., 2013). Well-developed gypsoliths are observed in sections 2 and 4 of the Lower Triassic Jialingjiang formation and in section 2 of the Middle Triassic Leikoupo formation (Figure 2) in the Puguang structure, thereby constituting the high-quality regional seal strata of the Changxing–Feixianguan formation gas reservoirs in this area. These gypsoliths possess great plasticity and maintain lateral continuity under the influence of tectonic stress; therefore, the gypsoliths also have a remarkable sealing capability (Ma et al., 2007a) to protect the petroleum reservoirs from uplifting and deformation since the late Cretaceous era. In this case, the hydrocarbon generation from source rocks has a well-configured relationship with reservoir–seal evolution for the petroleum accumulation. In addition, the crude oil cracking gas in the Lower Triassic reservoir (Lu et al., 2005) reached its production peak during the Cretaceous era and resulted from the formation of gypsolith seal rocks. All these conditions were proven favorable for the preservation of cracking gas.

3.2 Thermal regime changing with hydrocarbon generation and preservation

The end of the Cretaceous era resulted in uplifting and denudation in the Puguang area as well as reduced the geothermal gradient to reveal the complex processes of uplift, denudation, and basin cooling (Figures 5 and 6). Consequently, the strata temperature decreased and the Triassic temperature decreased between 80 °C and 120 °C (Figure 7). The relatively low temperature and geothermal gradient in this area (with an average value of ~20 °C/km) (Lu et al., 2005; Xu et al., 2011) favored the preservation of gas reservoirs and ensured the existence of hydrocarbon in deep strata. Therefore, in terms of geothermics, either the configuration of the hydrocarbon generation timing of source rocks and reservoir cap development or the low geothermal field background after the formation of cracked gas provided favorable conditions for hydrocarbon accumulation in the northeastern Sichuan basin.

The Silurian and Permian shale gas and source rock gas resources in this region have also attracted attention over the recent years (Huang et al., 2012; Liu et al., 2013; Gong et al., 2014). Temperature evolution affects the development of organic matter pores in strata and their gas adsorption capacity. In sum, a higher temperature and a greater extent of thermal evolution will result in highly developed organic matter pores (Jarvie et al., 2007; Loucks et al., 2009; Schieber, 2011), whereas a lower temperature will enhance the gas adsorption capacity (Ross and Bustin, 2007; Feng et al., 2012). As shown in Figure 7, the high temperature of the Permian source rocks, which may be attributed to the higher temperature gradient and

deepest burying level of these rocks before their denudation in the late Cretaceous era, was highly favorable for the maturity of organic matters and the development of their pores, whereas the cooling process after the main hydrocarbon and oil cracking gas generation periods benefited the preservation of source rock gas (shale gas).

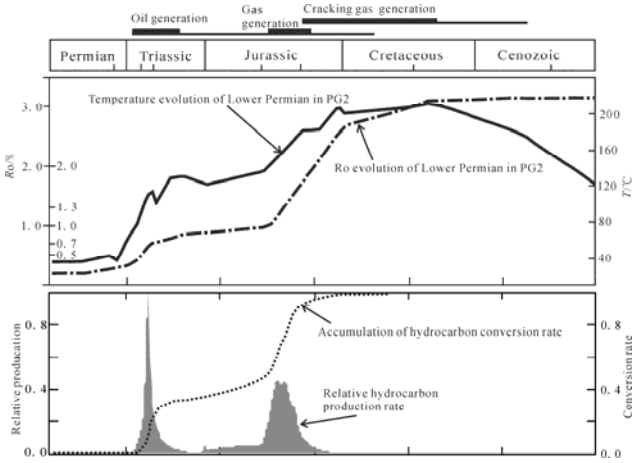

Figure 8 Thermal evolution and hydrocarbon generation history of the Permian source rock of PG2.

4. CONCLUSIONS

(1) The AFT modeling result indicates that except for slight cooling at approximately 140 Ma to 130 Ma, the Puguang area has experienced continuous burial and warming processes since the Jurassic era to 90 ± 10 Ma. After the maximum paleotemperature reached ~90 Ma, the cooling commenced and continued, which indicated the lasting uplift and denudation processes of northeastern Sichuan since the late Cretaceous era.

(2) The maximum paleotemperature reconstruction indicates that when the strata reach the maximum temperature, the geothermal gradient is approximately 30 °C/km and the erosion thickness is approximately 2.7 ± 0.2 km. The paleogeothermal gradient and paleo-heat flow were higher than their current values, thereby indicating the continuous uplifting and cooling processes in the basin since the late Cretaceous era.

(3) The Jurassic era was one of the most significant hydrocarbon generation periods for Silurian and Permian source rocks during which the thermal evolution entered into a post-maturity phase (dry gas stage) instead of an oil generating peak in the Triassic era. The thermal evolution process (warming and hydrocarbon generation followed by cooling after the formation of a reservoir cap system) of the source rocks in the northeastern Sichuan basin provided the necessary geothermal conditions for the accumulation of conventional oil-gas and unconventional hydrocarbon, such as shale gas.

ACKNOWLEDGMENTS

We would like to acknowledge comments from two anonymous reviewers and the suggestions provided by the editors. This study was supported by the National Key Basic Research Development Plan of China (Grant No. 2012CB214703), the National Natural Science Foundation of China (Grant No.41102152), the PetroChina Innovation Foundation (Grant No. 2013D-5006-0102) and the Science Foundation of China University of Petroleum, Beijing (Grant No. YJRC2013- 002).

REFERENCES CITED

Armstrong, P. A., Kamp, P. J. J., Allis. et al. 1997.Thermal effects of intrusion below the Taranaki Basin (New Zealand): evidence from combined apatite fission track age and vitrinite reflectance data. Basin Research, 9(2): 151-169.

Armstrong, P. A. 2005.Thermochronometers in Sedimentary Basins. Reviews in mineralogy and geochemistry, 58(1): 499-525.

Bray, R. J., Green, P. F., Duddy, I. R. 1992. Thermal history reconstruction using apatite fission track analysis and vitrinite reflectance: a case study from the UK East Midlands and Southern North Sea. Geological Society, London, Special Publications, 67(1): 3-25.

Burnham, A. K., Braun, R. L., Gregg, H. R., et al. 1987. Comparison of methods for measureing kerogen pyrolysis rates and fitting kinetic parameters. Energy & Fuels, 1: 452-458.

Burnham, A. K., Oh, M. S., Craford, R. W. 1989. Pyrolysis of Argonne Premium Coals: Activation Energy Distribution and related chemistry. Energy & Fuels, 3(1): 42-55.

Burnham, A. K., Sweeney, J. J. 1989. A chemical kinetic model of vitrinite maturation and reflectance. Geochimica et Cosmochimica Acta, 53(10), 2649-2657.

Cai, L. G., Rao, D., Pan, W. L., et al.2005.The evolution model of the Puguang gas field in northeast of Sichuan. Petroleum Geology & Experiment,27(5):462-467.

Corrigan, J. 1991. Inversion of apatite fission track data for thermal history information. Journal of Geophysical Research, 96, 347-360.

David, D., Antia, J. 1986. Kinetic method for modeling vitrinite reflectance. Geology, 14(7): 606-608.

Duddy, I. R., Green, P. F., Lastett, G. M. 1988. Thermal annealing of fission tracks in apatite,3.Aariable temperature behaviour. Chemical Geology, 73: 25-38.

Feng, Y. Y., Chu, W., Sun, W. J.2012. Adsorption characteristics of methane on coal under reservoir temperatures. Journal of China Coal Society, 37(9):1488-1492.

Fitzgerald, P. G., Gleadow, A. J. W.1990. New approaches in fission track geochronology as a tectonic tool: Examples from the transantarctic mountains. International Journal of Radiation Applications and Instrumentation. Part D. Nuclear Tracks and Radiation Measurements,17(3): 351-357.

Fitzgerald, P. G., Stump E., Redfield, T. F.1993. Late Cenozoic Uplift of Denali and Its Relation to Relative Plate Motion and Fault Morphology. Science, 259(5094): 497-499

Gallagher, K. 1995. Evolving temperature histories from apatite fission-track data. Earth Planet Science Letters, 136: 421-435.

Gleadow, A. J. W., Duddy, I. R., Green, P. F. et al. 1983.Fission track analysis: a new tool for the evaluation of thermal histories and hydrocarbon potential. Australian Petroleum Exploration Association Journal, 23: 93-102.

Gleadow, A. J. W., Fitzgerald, P. G.1987. Uplift history and structure of the Transantarctic Mountains: new evidence from fission track dating of basement apatites in the Dry Valleys area southern Victoria Land. Earth and Planetary Science Letters, 82(1-2): 1-14.

Gleadow, A. J. W. 1981. Fission-track dating methods: What are the real alternatives?. Nuclear Tracks, 5(1-2): 3-14.

Gong, L., Wang, C. Y., Yang, Y. G., et al.2014.Comparion of reservoir-forming conditions and objective exploration zones of shale gas in lower Silurian Longmaxi formation of Southwest and Northeast Sichuan Basin. Geological Science and Technology Information, 33(5):128-133.

Green, P. F., Duddy, I. R., Gleadow, A. J. W., et al. 1985. Fission track annealing in apatite: track length measurements and the form of the Arrhenius Plot. Nuclear Tracks,10,323-328.

Green, P. F., Duddy, I. R., Gleadow, A. J. W., et al. 1986. Thermal annealing of fission tracks in apatite, 1.A qualitative description. Chemical Geology, 59:237-253.

He, L. J., Xu, H. H., Wang, J. Y. 2011.Thermal evolution and dynamic mechanism of the Sichuan Basin during the Early Permian-Middle Triassic. Science China Earth Sciences, 54(12): 1948-1954.Hu, S. B., Zhang, R. Y., Zhou, L. C. 1998. Methods of thermal history reconstruction for oil-gas basin. Petroleum Explorationist, 3(4):52-54.

Hu, S. B., Fu, M. X., Yang, S. C., et al. 2007. Palaeogeothermal response and record of Late Mesozoic lithospheric thinning in the eastern North China Craton. in: Zhai M G, Windley B F, Kusky T M, et al. (eds) Mesozoic Sub-Continental Lithospheric Thinning Under Eastern Asia. Geological Society, London, Special Publications, 280, 267–280.

Huang, J. Z., Chen, S. J., Song, J. R., et al.1996. Hydrocarbon source systems and formation of gas fields in Sichuan Basin.Science in China (Series D), 40(1): 32-42.

Huang, J. Z.2012.Prospect of source rock gas based on shale gas accumulation patterns: A cas study from the low Permian in the Sichuan Basin. Natural Gas Industry, 32(11):4-9.

Jarvie, D. M., Hill, R. J., Ruble, T. E., et al. 2007.Unconventional shale-gas systems:The Mississippian Barnett Shale of north-central Texas as one model for thermogenic shale-gas assessment. AAPG Bulletin, 91(4):475-499.

Ketcham, R. A., Donelick, R. A., Carlson, W. D. 1999. Variabilityof apatitefission track annealing kinetics: III. Extrapolation to geological timescales. American Mineralogist, 84 (9):1235-1255.

Ketcham, R. A. 2005. Forward and inverse modeling of low temperature thermochronometry data Reviews in Mineralogy and Geochemistry, 58, 275-314.

Ketcham, R. A., Carter, A., Donelick, R. A., et al. 2007.Improved modeling of fission-trackannealing in apatite. Am. Mineral., 92, 799-810.

Larter, S. 1989. Chemical models of vitrinite reflectance evolution. Geologische Rundschau,78(1) :349-359.

Lerche, I., Yarzab, R. F., Kendall, C. G. 1984. Determination of paleoheat flux from vitrinite reflectance data. AAPG Bulletin, 68(11): 1704-1717.

Lerche, I. 1990. Basin Analysis: Quantitative Methods Volume I. San Diego: Academic Press Inc, 74-96.

Liang, D. G., Guo, T. L., Chen, J. P., et al.2008.Distribution of four suits of regional marine source rocks. Marine Petroleum Geology, 13(2):1-16.16

Liu, D. H., Xiao, X. M., Tian, H., et al.2013.Multiple types of high density methane inclusions and their relationships with exploration and assessment of oil-cracked gas and shale gas discovered in NE Sichuan. Earth Science Frontiers, 20(1):64-71.

Loucks, R. G., Reed, R. M., Ruppel, S. C., et al. 2009.Morphology, genesis, and distribution of nanometer-scale pores in siliceous mudstones of the Mississippian Barnett Shale. Journal of Sedimentary Research, 79(12):848-861.

Lu, Q. Z., Hu, S. B., Guo, T. L.,et al. 2005.The background of the geothermal field for formation of abnormal high pressure in the northeastern Sichuan Basin. Chinese Journal of Geophysics, 48, 1110-1116.

Lutz, T. M., Omar, G. 1991. Inverse methods of modeling thermal histories from apatite fission track data. Earth Planet Science Letters, 104:181-195.

Ma, Y. S., Cai, X. Y., Guo, T. L., et al.2007a.The controlling factors of oil and gas charging and accumulation of Puguang gas field in the Sichuan Basin. Chinese Science Bulletin, 52 (Supp. I):193-200.

Ma, Y. S., Guo, X. S., Guo, T. L., et al.2007b.The Puguang gas field: New giant discovery in the mature Sichuan Basin, southwest China. AAPG Bulletin, 91, 627-643.

Ma, Y. S.2010.Formation Mechanism of Deep-Buried Carbonate Reservoir and Its Model of Three-Element Controll ing Reservoir: A Case Study from the Puguang Oi lfield in Sichuan. Acta Geologica Sinica, 84(8):1087-1094.

Mei, L. F., Liu, Z. Q., Tang, J. G., et al.2010.Mesozoic Intra-Continental Progressive Deformation in Western Hunan-Hubei Eastern Sichuan Provinces of China: Evidence from Apatite Fission Track and Balanced Cross-Section. Earth Science-Journal of China University of Geosciences, 35(2): 161-174.

Naeser, C. W. 1979.Thermal history of sedimentary basins: fission track dating of subsurface rocks. In: Scholle P A and Schluger P R Eds. Aspects of Diagenesis. Society of Economic Paleotologists and Mineralogists Special Publication, 26:109-112.

O'Sullivan, P. B. 1999. Thermochronology, denudation and variations in palaeosurface temperature: A case study from the North Slope foreland basin, Alaska. Basin Research, 11: 191–204.

Rao, S., Tang, X. Y., Zhu, C. Q., et al. 2011. The application of sensitivity analysis in the source rock maturity history simulation: An example from Palaozioc marine source rock of Puguang-5 well in the northeast of Sichuan Basin. Chinese journal of geology, 46(1): 213-225.

Qiu, N. S., Qin, J. Z., Brent, I. A. M.2008.Tectonothermal evolution of the northeastern Sichuan basin: Constraints from apatite and zircon (U-Th)/He ages and vitrinite

reflectance data. Geological Journal of Chinese Universities, 14, 223-230.

Rao, S., Zhu, C. Q., Wang, Q., et al.2013. Thermal evolution patterns of the Sinian-Lower Paleozoic source rocks in the Sichuan basin, sourthwest China. Chinese Journal of Geophysics, 56(5):1549-1559.

Ross. D. J. K., Bustin, R. M. 2007. Shale gas potential of the lower jurassic gordondale member, northeastern British Columbia, Canada. Bulletin of Canadian Petroleum Geology, 55(1):51-75.

Schieber. J. 2011. Shale microfabrics and pore development: an overview with emphasis on the importance of depositional processes. Gas Shale of the Horn River basin, 115-119.

Shen, C. B., Mei, L. F., Guo T L.2007.Fission track analysis of Mesozoic-Cenozoic thermal history in northeast Sichuan Basin, Natural Gas Industry, 27, 24-26.

Sweeney, J. J., Burnham, A. K. 1990. Evaluation of a simple model of vitrinite reflectance based on chemical kinetics. AAPG Bulletin, 74: 1559-1570.

Tenger, Liu, W. H., Qin, J. Z., et al. 2012. Dynamic transformation mechanism forhydrocarbon generation from multiple sources in deep-buried marine carbonates in the northeastern Sichuan Basin: A casestudy from the Puguang gas field. Acta Petrologica Sinica, 28(3) : 895-904.

Tenger, Qin, J. Z., Fu, X. D., et al.2010.Hydrocarbon source rocks evaluation of the Upper Permian Wujiaping Formation in northeast Sichuan area. Journal of Palaeogeography, 12(3):1-12.

Tian, Y. T., Zhu, C. Q., Xu, M., et al.2011.Post-Early Cretaceous denudation history of the northeastern Sichuan Basin: constraints from low-temperature thermochronology profiles. Chinese Journal Geophysics, 54(3): 807-816.

Tian. Y. T., Kohn, B. P., Zhu, C. Q., et al.2012.Post-orogenic evolution of the Mesozoic Micang Shan Foreland Basin system, central China. Basin Research, 24, 70-90.

Tissot, B. P., Pelect, R. U. 1987. Thermal History of Sedimentary Basin Maturation Indices and Kinetics of Oil and Gas Generation. AAPG Bulletin, 71: 1445-1466.

Tissot, B. P., Welte, D. H. 1984. Petroleum Formation and Occurrence. New-York: Springer Verlag.

Tissot, B., Espitalie, J. 1975. L'evolution thernique de la matiere organique des sediments: Applications dune simulation mathematique. Oil & Gas Science and Technology, 30: 743-778.

Wu, Q., Peng, J. N.2013.Burial and thermal histories of northeastern Sichuan Basin:A case study of well Puguang 2.Petroleum Geology & Experiment, 35(2):133-138.

Xu, M., Zhu, C. Q., Tian, Y. T., et al.2011.Well temperature logging and characteristics of subsurface temperature in Sichuan Basin. Chinese Journal of Geophysics, 54, 1052-1060.

Zhang, G. C.2014.Analysis of the regular distribution of oil and gas fields in China based on the theory of hydrocarbon generation controlled by source rocks and geothermal heat. Natural Gas Industry, 34(5):1-28.

Zhang, G. C.2012.Co-control of source and heat: the generation and distribution of hydrocarbons controlled by source rocks and heat. Acta Petrolei Sinica. 33(5):723-738.

Zheng, R. C., Geng, W., Zheng, C., et al.2008. Genesis of dolostone reservoir of Feixianguan Formation in Lower Triassic of northeast Sichuan Basin, Acta Petrolei Sinica,29(6):815-821.

Zhou, Y., Jin, Z. J., Zhu, D. Y., et al.2013b. Current status and progress in research of hydrocarbon cap rocks. Petroleum Geology & Experiment, 34(3):234-245.

Zhu, C. Q., Xu, M., Yuan, Y. S., et al. 2010a.Paleogeothermal response and record of the effusing of Emeishan basalts in the Sichuan basin. Chinese Science Bulletin, 55(10): 949-956.

Zhu, C. Q., Tian, Y. T., Xu, M., et al. 2010b. The effect of Emeishan supper mantle plume to the thermal evolution of source rocks in the Sichuan basin. Chinese Journal of Geophysics, 53(1): 119- 127.

Zhu, C. Q., Hu S. B., Qiu, N. S., et al. 2016. Thermal history of the Sichuan Basin, SW China: Evidence from deep boreholes. Science China: Earth Sciences, 59(1): 70–82.